JOURNAL OF AIRCRAFT
Vol. 30, No. 6, Nov.–Dec. 1993

Aerothermodynamic Properties of Hypersonic Flow over Radiation-Adiabatic Surfaces

Stefan Riedelbauch*
Deutsche Forschungsanstalt für Luft- und Raumfahrt, D-3400 Göttingen, Germany
and
Ernst H. Hirschel†
Messerschmitt-Bölkow-Blohm GmbH, D-8000 München 80, Germany

The aerothermodynamic properties of hypersonic flow over radiation-adiabatic walls (radiation-cooled adiabatic walls) are investigated by the numerical simulation of the viscous flowfield past a delta wing with blunt leading edges. Surface-radiation cooling is an effective technique to reduce the heat loads of airplanes flying at hypersonic speed. The simulated flowfields are analyzed in detail, focusing on the heat load distribution of the wing flying at a freestream Mach number of 7.15 and an angle of incidence of 15 deg. Locally increased surface temperatures appear close to attachment lines on the wing. On the leeward side this effect is due to vortex/boundary-layer interaction. The radiation-adiabatic surface temperature is compared with computed results of adiabatic wall, revealing a considerable cooling effect, and with results obtained by an approximate method. The influence of the variation of length scales on the radiation-adiabatic surface temperature is discussed, and it is shown that a scaling of the radiation-cooled adiabatic wall temperature between bodies of different size, e.g., wind-tunnel model/experimental vehicle/real size airplane, is possible for laminar flow.

Introduction

A TYPICAL problem of airplanes for hypersonic flight (e.g., Space Shuttle, Hermes, Nasp, Sänger, and others) are the high heat loads on the structure.[1] A considerable part of the kinetic energy of the airplane is transformed into heat by compression and viscous effects. This heat is transported to the surface by heat conduction and causes high temperature levels and/or large heat fluxes there (here, "heat loads" means both surface temperatures and associated heat fluxes). Owing to vortex impingement, aerodynamic heating on local areas of the leeward surface of the Space Shuttle was higher than expected during re-entry.[2] Wind-tunnel experiments were carried out by Bertin and Goodrich[3] investigating the influence of the surface temperature and the Reynolds number on the heat load of the leeward side of the Space Shuttle.

The effect of radiation cooling is shown in Fig. 1. These results were obtained with an approximate method for a certain point on the windward side of a hypersonic airplane, taking into account surface radiation cooling. Different freestream Mach numbers corresponding to a certain flight trajectory were chosen as parameter; turbulent flow was assumed. Specially marked are the total temperature T_0, the recovery temperature T_r, and the radiation-adiabatic wall temperature T_{ra}. It is obvious that surface radiation diminishes the wall temperature T as well as the heat flux into the structure q_w. The cooling effect due to radiation is very small for low-temperature values, but becomes more and more pronounced with increasing temperature levels.

In this article the aerothermodynamic properties of hypersonic flow past radiation-adiabatic surfaces are investigated. The emphasis lies on numerical experiments by means of solutions of the Navier-Stokes equations for the flow past a delta wing with a blunt leading edge. Initially, a local analysis[4] of the radiation-adiabatic wall temperature is repeated in order to formulate the basic problem. The radiation-adiabatic temperature is a conservative estimation like the recovery temperature. In contrast to the recovery temperature, it depends on some local characteristic length, and hence, on a global length scale and on the global Reynolds number. This leads to special phenomena connected to vortex/boundary-layer interactions, especially at the leeward side of vehicles, which are studied here. Of course, this also leads to a transfer problem of data from small configurations (wind-tunnel model, experimental vehicle) to full-size vehicles. This problem is also investigated here.

During the design of hypersonic airplanes, a large number of computations have to be performed to determine the heat loads to study parameter variations for optimization reasons. The use of approximate methods permits a much faster computation of these heat loads compared to a Navier-Stokes flowfield simulation. However, they make use of approximate

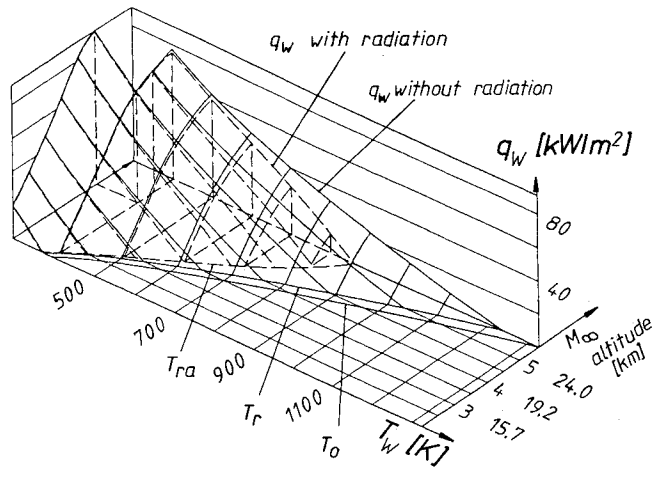

Fig. 1 Influence of surface radiation on the wall temperature and the heat flux into the structure for a point on the windward symmetry plane of a hypersonic airplane at different trajectory points (M_∞-altitude).[4]

Received April 30, 1992; revision received Aug. 4, 1992; accepted for publication Aug. 4, 1992.

*Research Engineer, Institute of Theoretical Fluid Mechanics, Bunsenstraße 10.

†Manager, Technology Air Vehicle Engineering, Unternehmensbereich Flugzeuge, Postfach 801160. Member AIAA.

relations and empirical formulas, which do not always yield a sufficient good approximation of the flow under consideration. In order to assess such methods, a comparison between results obtained by an approximate method[5] and a Navier-Stokes computation is carried out.

The flow assumes laminar and perfect gas. Turbulence and high-temperature effects are not considered because it is intended to show only the basic effects and phenomena related to radiation-adiabatic surfaces. The emission and absorption of radiation energy in air is neglected because these heat quantities are small at speeds below $\tilde{v}_\infty \approx 8$ km/s.[6] Radiation energy of the sun is also neglected.

In the following chapter, the heat loads at a radiation-adiabatic surface are discussed qualitatively. Then, the governing equations and the numerical method are outlined, and finally, results with regard to the above-mentioned subjects are presented.

Heat Loads at a Radiation-Adiabatic Surface

To discuss the heat loads, the local heat flux balance at the body surface is considered. Owing to the viscous forces in the boundary layer, the flow velocity is reduced from the edge value to zero at the wall corresponding to the no-slip condition. Thus, only heat conduction transfers heat between fluid and body surface. This is described by Fourier's law $\tilde{q}_{gw} = -\tilde{\kappa}\partial\tilde{T}/\partial\tilde{n}|_{\tilde{n}=0}$. Due to radiation, the surface looses energy to "infinity." This can be considered as heat sink. The corresponding heat flux is determined by the Stefan-Boltzmann law $\tilde{q}_{\mathrm{ra}} = \tilde{\sigma}\varepsilon\tilde{T}^4$, where $\tilde{\sigma}$ denotes the Stefan-Boltzmann constant and ε the emission coefficient ($0 \leq \varepsilon \leq 1$). The heat flux being conducted into the structure is given by $\tilde{q}_w = -\tilde{\kappa}_{\mathrm{st}}\partial\tilde{T}/\partial\tilde{n}|_{\mathrm{structure}}$. The resulting heat flux balance at the body surface

$$\tilde{q}_{gw} + \tilde{q}_{\mathrm{ra}} + \tilde{q}_w = 0 \tag{1}$$

couples the temperature distribution of the flowfield with that of the structure. Equation (1) is only valid for convex geometries. That means that parts of the radiating surface may not face each other, otherwise that has also to be taken into account. Various boundary conditions can be distinguished for the wall temperature using Eq. (1).[4] A special case is the radiation-adiabatic wall, which corresponds to the condition that the heat flux into the structure is zero, i.e., $\tilde{q}_w = 0$. This estimate is the largest possible wall temperature, which has to be expected for the surface. Without radiation cooling, the much larger recovery temperature will occur at the surface.

In the following, the radiation-adiabatic wall temperature is discussed qualitatively. The condition for the radiation-adiabatic wall reads

$$-\tilde{\kappa}\left.\frac{\partial\tilde{T}}{\partial\tilde{n}}\right|_{\tilde{n}=0} + \varepsilon\tilde{\sigma}\tilde{T}_{\mathrm{ra}}^4 = 0 \tag{2}$$

The temperature gradient at the wall can be approximated by

$$\left.\frac{\partial\tilde{T}}{\partial\tilde{n}}\right|_{\tilde{n}=0} \approx \frac{\tilde{T}_{0,\infty} - \tilde{T}_{\mathrm{ra}}}{\tilde{\Delta}} \tag{3}$$

where $\tilde{\Delta}$ denotes some characteristic thickness of the boundary layer, and $\tilde{T}_{0,\infty}$ the total temperature of the flow at freestream conditions. Assuming a laminar flat plate boundary-layer flow and that $\tilde{\Delta} = \tilde{\delta}_T$, the thickness of the temperature boundary layer, the following relations hold[7]:

$$\frac{\tilde{\delta}_T}{\tilde{x}} \sim \frac{1}{Pr^{0.5}Re_{\infty,x}^{0.5}}, \quad Re_{\infty,x} = \frac{\tilde{x}}{\tilde{L}}Re_{\infty,L} \tag{4}$$

After inserting Eqs. (3) and (4) in Eq. (2), the qualitative dependency of the radiation-adiabatic wall temperature is obtained to be

$$\tilde{T}_{\mathrm{ra}}^4 \sim \frac{\tilde{\kappa}}{\varepsilon\tilde{\sigma}}\frac{Pr_\infty^{0.5}}{\tilde{\delta}_s}\tilde{T}_{0,\infty}\left(1 - \frac{\tilde{T}_{\mathrm{ra}}}{\tilde{T}_{0,\infty}}\right)\Bigg|_{\tilde{n}=0} \tag{5a}$$

or

$$\tilde{T}_{\mathrm{ra}}^4 \sim \frac{\tilde{\kappa}}{\varepsilon\tilde{\sigma}}\frac{Pr_\infty^{0.5}Re_{\infty,L}^{0.5}}{(\tilde{x}/\tilde{L})^{0.5}}\frac{\tilde{T}_{0,\infty}}{\tilde{L}}\left(1 - \frac{\tilde{T}_{\mathrm{ra}}}{\tilde{T}_{0,\infty}}\right)\Bigg|_{\tilde{n}=0} \tag{5b}$$

where $\tilde{x}$ denotes the running length, $\tilde{L}$ the characteristic length of the problem, $Re_{\infty,L}$ the global Reynolds number, Pr_∞ the Prandtl number at freestream conditions, $\tilde{T}_{\mathrm{ra}}$ the radiation-adiabatic surface temperature and $\tilde{\delta}_s$ the boundary-layer thickness for laminar flow. Equation (5b) is obtained assuming the proportionality[7] $\tilde{\delta}_T/\tilde{\delta}_s \sim 1/\sqrt{Pr_\infty}$.

Equation (5) shows that a scale dependency exists. The radiation-cooled adiabatic surface temperature of a body can be scaled to another body, provided the surface flow topology is the same in both cases. The flowfields may have different freestream conditions and emission coefficients ε which may vary for different materials. The different cases are denoted with states 1 and 2. The radiation-adiabatic surface temperature can be estimated for each state using Eq. (5). Then, at every position $\tilde{x}/\tilde{L}$, the following expression is obtained for the temperature ratio:

$$\frac{\tilde{T}_{\mathrm{ra},1}^4}{\tilde{T}_{\mathrm{ra},2}^4} \sim \frac{\left[\frac{\tilde{\kappa}}{\varepsilon\tilde{\sigma}}Pr_\infty^{0.5}Re_{\infty,L}^{0.5}\frac{1}{\tilde{L}}(\tilde{T}_{0,\infty} - \tilde{T}_{\mathrm{ra}})\right]_1}{\left[\frac{\tilde{\kappa}}{\varepsilon\tilde{\sigma}}Pr_\infty^{0.5}Re_{\infty,L}^{0.5}\frac{1}{\tilde{L}}(\tilde{T}_{0,\infty} - \tilde{T}_{\mathrm{ra}})\right]_2} \tag{6}$$

The above formula [Eq. (6)] allows the estimation of changes of the radiation-adiabatic wall temperature due to differences of characteristic freestream conditions and lengths of geometric similar bodies.

An exclusive change of the characteristic lengths, together with the following assumptions:

$$[\tilde{T}_{0,\infty} - \tilde{T}_{\mathrm{ra}}]_1 \approx [\tilde{T}_{0,\infty} - \tilde{T}_{\mathrm{ra}}]_2 \tag{7a}$$

$$[\tilde{\kappa}]_1 \approx [\tilde{\kappa}]_2 \tag{7b}$$

yields

$$(\tilde{T}_{\mathrm{ra},1}^4/\tilde{T}_{\mathrm{ra},2}^4) \sim (\tilde{L}_2/\tilde{L}_1)^{0.5} \tag{8}$$

A shortening of the characteristic length, e.g., the wing length, results in an increase of the radiation-adiabatic wall temperature.

Governing Equations and Numerical Method

The basic equations under consideration are the unsteady thin-layer Navier-Stokes equations written in conservative form for a body-fitted coordinate system. The physical domain considered is bounded by the body, the inflow surface, and the upper and lower symmetry planes, as well as the outflow plane. Standard boundary conditions are applied.

The numerical method used here is based on a finite difference formulation in which the inviscid fluxes are discretized according to Harten and Yee's upwind "total variation diminishing" shock-capturing scheme.[8] Formal second-order accuracy is obtained by means of the nonMUSCL approach. For the viscous fluxes, a central discretization is employed. The conservative finite-difference scheme employs an implicit evaluation of the time derivative to first-order, resulting in a line Gauß-Seidel relaxation method. Details and equations of the numerical scheme are presented, e.g., in Refs. 9 and 10.

Several comparisons have been carried out with experimental and other numerical investigations. For those com-

parisons, the upwind scheme and the basic algorithm with central discretization have been checked. Many of the comparisons with the central scheme are documented, e.g., in Refs. 11 and 12 and with the upwind TVD scheme in Refs. 9, 13, and 14. In general, a good agreement has been obtained.

Results

Hypersonic flows past a delta wing with radiation-adiabatic wall are numerically simulated. The specific geometry of the delta wing, Fig. 2, with blunt leading edges was chosen, because the projected wing area roughly corresponds to that of a hypersonic spaceplane and, additionally, results from experimental investigations are available[15] for validation purposes. These experiments were carried out for the "Workshop on Hypersonic Flows for Reentry Problems," which was held in 1990 and 1991 in Antibes, France. For an altitude $H = 30$ km, the atmospheric state reads: $\bar{T}_\infty = 226.5$ K, $\bar{p}_\infty = 1197$ N/m^2, $\bar{\rho}_\infty = 0.01841$ kg/m^3, $\bar{\mu}_\infty = 1.4753\ 10^{-5}$ kg/ms, $\bar{\kappa}_\infty = 2.0345\ 10^{-2}$ N/sK, $\bar{c}_p/\bar{c}_v = 1.4$. Corresponding to the wind-tunnel experiments,[15] the freestream Mach number amounts to $M_\infty = 7.15$, accordingly the freestream velocity is $\bar{u}_\infty = 2157$ m/s. The angle of incidence is $\alpha = 15$ deg. The Prandtl number is $Pr_\infty = 0.728$ and the Reynolds number per meter $Re_\infty/m = 2.69\ 10^6$. For the emission coefficient of the body surface $\varepsilon = 0.85$ is assumed, while the Stefan-Boltzmann constant is $\bar{\sigma} = 5.67032\ 10^{-8}$ W/m^{2}K^4. The corresponding flight condition lies close to that of the Sänger lower stage, and a little bit further away from the re-entry trajectory of space planes like the Space Shuttle/Hermes.

Navier-Stokes solutions were obtained for a wing length of $L = 14$ m and of $L = 4.67$ m. The larger size corresponds to the Hermes vehicle length, and the smaller size corresponds to that of a possible experimental vehicle. These solutions are used for scaling considerations. An Euler solution[9] provides the boundary-layer edge conditions needed to calculate aerodynamic heating when using approximate methods. A Navier-Stokes solution assuming an adiabatic wall with negligible radiation ($\bar{q}_w = \bar{q}_{gw} = \bar{q}_{ra} = 0$, $\bar{L} = 14$ m) has also been obtained.

The computational grid is built with algebraic methods and consists of $i \times j \times k = 121 \times 135 \times 61$ nodes (streamwise $\times$ circumferential $\times$ wall normal) with consideration of a symmetry plane. Selected grid surfaces being reflected about the symmetry plane are displayed in Fig. 3. They show the wing surface and three cross-sectional planes. The grid is iteratively adapted to the bow shock with the typical result that only four or five points are located in the freestream region at each ray in wall normal direction. This adaptation improves the resolution of the flowfield between body and bow shock for a fixed number of points.

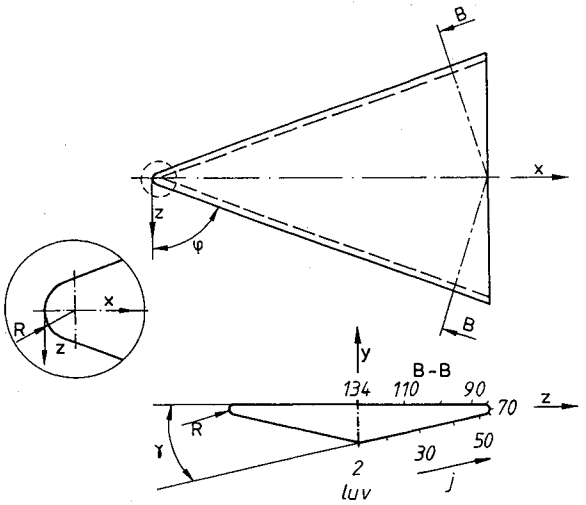

Fig. 2 Definition of the wing geometry and selected coordinate lines.

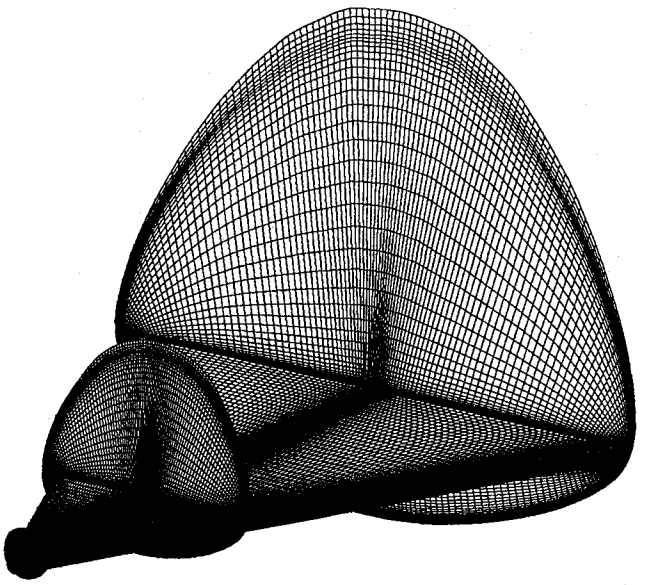

Fig. 3 Selected surfaces of the 121 × 135 × 61 adapted computational grid (grid reflected about symmetry plane).

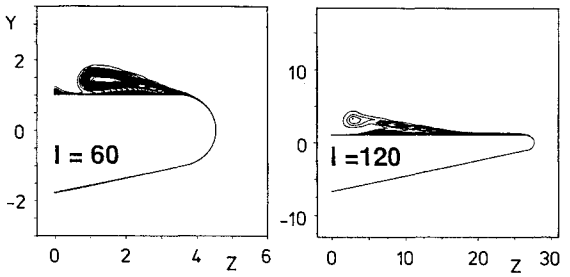

Fig. 4 Total enthalpy loss in the cross sections $i = 60$ ($x/L = 0.14$) and $i = 120$ ($x/L = 0.99$) ($M_\infty = 7.15$, $\alpha = 15$ deg, $Re_{\infty,L} = 37.7\ 10^6$).

Analysis of the Flowfield and the Thermal Surface State

The flow past the delta wing is characterized by a detached bow shock and separated flow on the leeward side. The bow shock stand-off distance is small along the supersonic leading edges and on the windward side, and comparatively large on the leeward side.

The total enthalpy H is a measure of the energy content of the flow. It is constant in the case of an inviscid flowfield, where deviations from this constant indicate errors of numerical nature. In the viscous case, however, the flowfield loses energy due to the radiation-adiabatic wall. The loss of energy can be measured by the total energy loss $\Delta H_v = (H_\infty - H)/H_\infty$, which exhibits gradients in a very narrow zone close to the wing being essentially the temperature boundary layer, and in the region of separation (Fig. 4). Outside the leeward vortex, and outside the temperature boundary layer, the total enthalpy loss is smaller than $\Delta H_v = 0.025$. This value corresponds to the first contour line plotted in Fig. 4. It becomes evident that fluid containing the energy level of the freestream comes close to the surface not only on the windward side, but also near the leeward symmetry plane.

The distribution of the heat loads as well as the skin-friction lines (black) are presented in Fig. 5 for the windward and the leeward side of the wing. The attachment lines along the leading edges are characteristic for the flowfield. There, with the exception of the stagnation region, the temperature is nearly constant and amounts to about 1100 K. On the windward side, the temperature does not drop below 750 K, while the maximum value in the stagnation region is about 1500 K. On the windward side, the skin-friction lines exhibit a very uniform behavior. Only near the windward symmetry plane

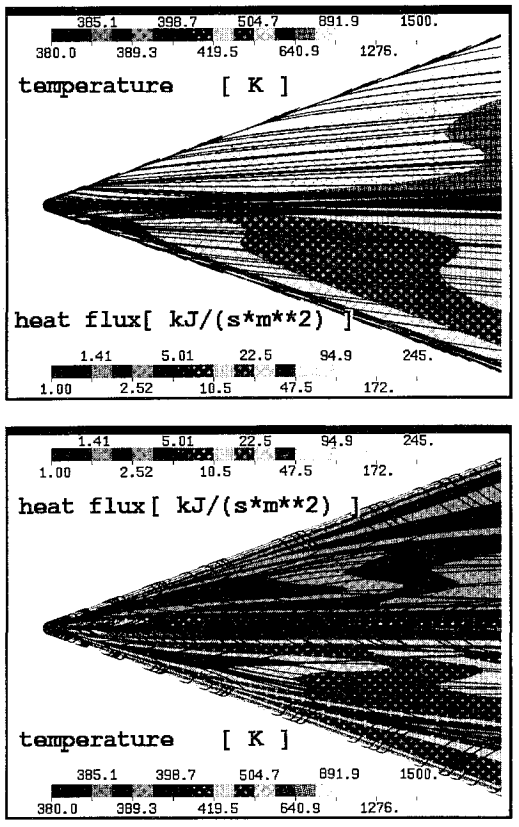

Fig. 5 Distribution of the radiation-adiabatic wall temperature and the corresponding heat flux as well as skin-friction lines on the windward (top) and leeward side (bottom) of the wing (M_∞ = 7.15, α = 15 deg, $Re_{\infty,L}$ = 37.7 10^6).

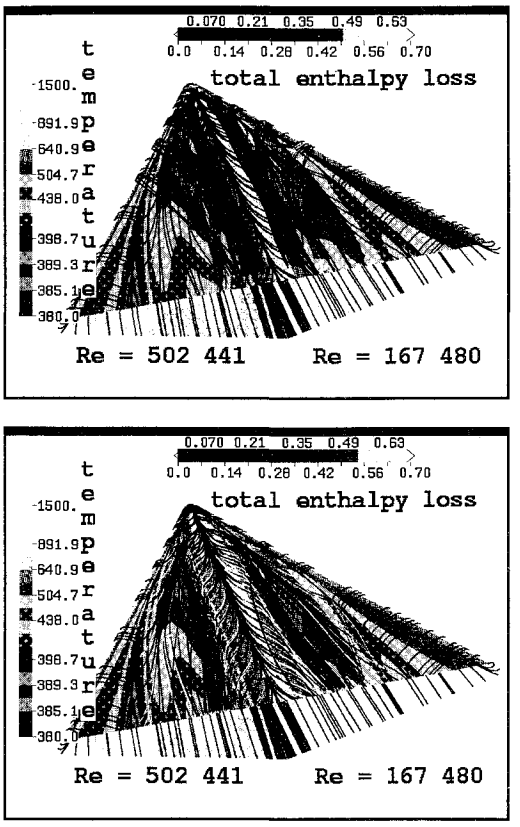

Fig. 6 Radiation-adiabatic surface temperature, skin-friction lines and selected streamlines with total enthalpy loss (wing viewed from rear). Left half of the picture: L = 14 m, right half of the wing: L = 4.67 m, primary vortex: top, secondary vortex: bottom (M_∞ = 7.15, α = 15 deg).

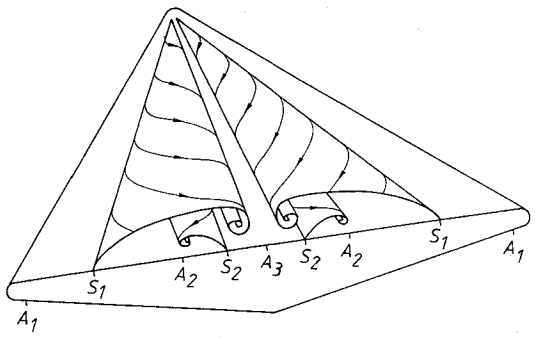

Fig. 7 Sketch of the topology of the flow past the delta wing (A = attachment lines, S = separation lines).

is a weak concentration of these lines observed, being caused by three-dimensional effects near the wing nose. The leeward side of the wing shows footprints of vortices. Flow separation, being characterized by converging skin-friction lines, locally leads to low values of the surface temperature, while attachment lines, being characterized by diverging skin-friction lines, clearly result in high values of the surface temperature. The reason for this is that at attachment lines the boundary layer becomes thin and at separation lines it becomes thick.[16] Therefore, according to Eq. (5a), the radiation adiabatic temperature becomes large or small, respectively.

In the following, the topological structure is determined to get a qualitative description of the separated flow.[17] Since the base flow of the wing is not considered, the skin-friction velocity vector field shows a singular point only in the stagnation point. The beginning of the separation lines exhibits the features of a so-called open separation. Selected streamlines show the primary vortices, which are located fairly close to the symmetry plane (Fig. 6). Another selection of the start points for the streamline integration visualizes the secondary vortices which rotate in opposite direction compared to the primary vortices. The results displayed on the left half of the wing (wing seen from behind) correspond to the wing length L = 14 m ($Re_{\infty,R}$ = 502,441 being equivalent to $Re_{\infty,L}$ = 37.7 × 10^6) and those on the right half of the wing belong to the wing length L = 4.67 m ($Re_{\infty,R}$ = 167,480 being equivalent to $Re_{\infty,L}$ = 12.6 × 10^6). In agreement with Eq. (8), the level of the radiation-adiabatic surface temperature is higher for the smaller wing. Now, the qualitative structure of the flowfield can be sketched, which is essentially similar for the large and the small wing (Fig. 7).

On the windward side of the wing, the skin-friction lines do not show a conical, but a two-dimensional behavior. Three-dimensional effects are only present in a narrow zone along the symmetry plane and along the attachment lines at the leading edges. Additionally, the pressure in main flow direction is nearly constant. These properties of the flow resemble those of a flat plate. Thus, the validity of the proportionality, Eq. (5), has to be expected. In fact, the radiation-adiabatic surface temperature decreases with increasing running length of the flow (Fig. 5). However, the entropy layer caused by the curved bow shock may change the boundary-layer profile compared to a flat plate flow.

To quantify the influence of leeward vortices on the radiation-adiabatic wall, the temperature distributions in the cross sections i = 60 and i = 120 are plotted in Fig. 8. Local minima of the temperature appear close to separation lines S, while local maxima appear close to attachment lines A. It can be shown that local maxima/minima do not necessarily coincide with attachment/separation lines. This means that their locations can be shifted against each other. This is the case in cross section i = 60 near the leeward symmetry plane. Here, the location of the local temperature maximum corresponds to the region where a thin temperature boundary layer occurs [cf. Fig. 4, Eq. (3)]. The local temperature maxima varies

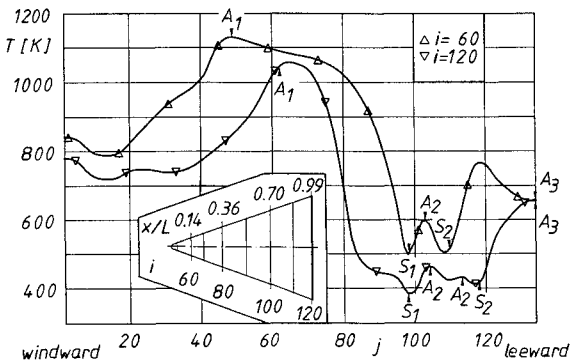

Fig. 8 Radiation-adiabatic wall temperature and location of separation and attachment lines in the cross sections $i = 60$ and $i = 120$ ($M_\infty = 7.15$, $\alpha = 15$ deg, $Re_{\infty,L} = 37.7\ 10^6$).

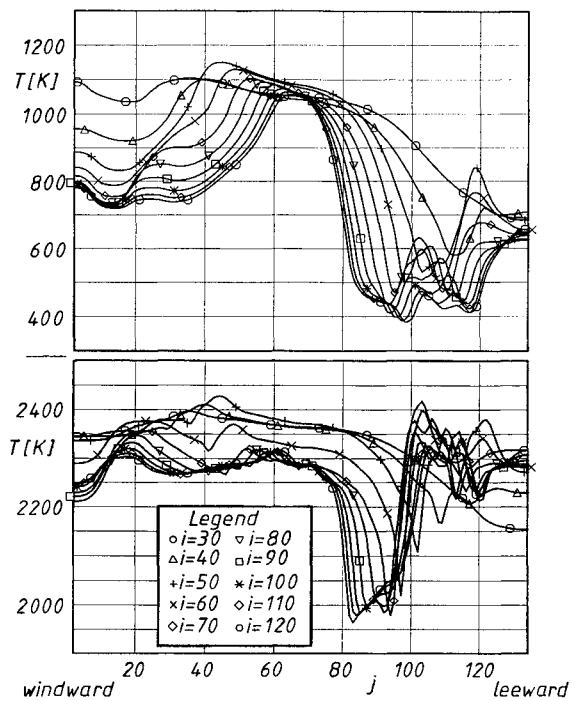

Fig. 9 Surface temperature in several cross sections for a radiation-adiabatic wall (top) and an adiabatic wall (bottom), ($M_\infty = 7.15$, $\alpha = 15$ deg, $Re_{\infty,L} = 37.7 \times 10^6$, $T_{0,\infty} = 2542.4$ K, recovery temperature for a flat plate $T_r = 2202.5$ K).

between 650–750 K due to the primary vortices, while the secondary vortices cause local maxima of the wall temperature of 450–600 K.

In principle, the influence of surface radiation on the temperature is presented in Fig. 1. To substantiate this effect and to show the quantitative difference, a flowfield computation is carried out assuming an adiabatic wall with negligible radiation ($\bar{q}_w = \bar{q}_{ra} = \bar{q}_{gw} = 0$). The adiabatic surface temperature is shown in Fig. 9 in different cross sections. In the adiabatic case, the temperature level is roughly 1400 K higher on the windward side, about 1200 K higher along the leading edges, and approximately 1700 K higher on the leeward side. The cooling effect of surface radiation is highest in the region dominated by secondary vortices. At $x/L \approx 0.45$, the attachment lines of the secondary vortices spread out (Fig. 5). Downstream of this location, the velocity vector points essentially in the main flow direction. The crossflow components are small (Fig. 6). Thus, the region between primary S_1 and secondary S_2 separation line can be considered to be a thin bubble which is weakly fed with flow containing high total enthalpy. Therefore, the surface below the secondary vortices is cooled down with increasing running length from about 600–400 K. The situation differs for the primary vortices. They transport flow with high total enthalpy towards the surface along the entire wing length. This results in a thin temperature boundary layer, and therefore, in increased temperature levels at and near the symmetry plane (Figs. 4–6). The comparison of both flowfields illustrates the considerable cooling effect of surface radiation.

Comparison with an Approximate Method

The approximate method requires local flow conditions at the boundary-layer edge, as well as the local running length of an inviscid streamline. This is provided by an Euler solution on a 121 × 69 × 37 grid neglecting the displacement effect of the boundary layer.[9] The radiation-adiabatic temperatures are only determined at locations $j = 8, 18, \ldots, 68$ using the approximate method.

The qualitative behavior of both results is similar (Figs. 9 and 10), except for the fact that the attachment-line heating is not found. In general, the approximate method underpredicts the surface temperature along the leading edges and on the windward side of the wing. One possible cause for this effect is the entropy layer, which is swallowed by the boundary layer to a certain degree. Investigations being presented in Ref. 18 have shown that the consideration of the entropy-layer swallowing effect increases the heat loads. Thus, the consideration of this effect should lead to an improvement of the prediction capabilities of approximate methods.

However, the use of approximate methods on the leeward side of airplanes has to be considered very critical. Their nearness to reality is essentially dependent on whether the flow is separated, which is influenced by the body geometry and the freestream conditions. Flow separation can already occur at low angles of incidence. In the case of attached flow on the leeward side, results can be expected that are qualitatively and quantitatively similar to those presented above for the windward side of the delta wing. In the case of separation, the flow cannot be predicted correctly using an inviscid model. Therefore, approximate methods fail in such flow regions. The accurate prediction of the radiation-adiabatic wall temperature on the leeward side requires the simulation of the complete viscous flowfield. This is not only necessary for large angles of incidence, but also for small ones, because the knowledge of the inviscid flow alone does not allow decisions on a physical basis whether the flow is separated or not. Such a criterion can possibly be furnished by coupled Euler/boundary-layer methods.

Similarity Considerations

During the development phase of hypersonic airplanes, the thermal loads have to be determined. Results, obtained by means of wind-tunnel models and/or by experimental airplanes, have to be carried over to each other and to the final airplane. In the following, it is shown how a reduction of the

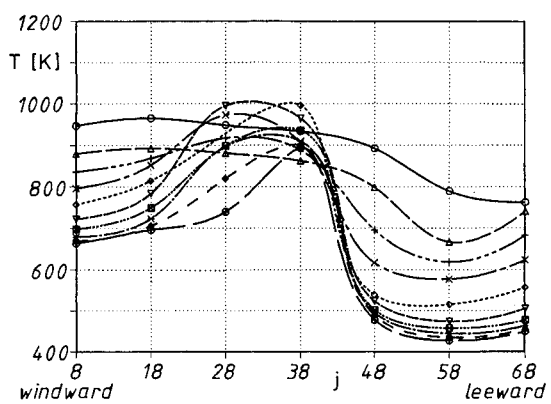

Fig. 10 Radiation-adiabatic surface temperature of the approximate method in several cross sections ($M_\infty = 7.15$, $\alpha = 15$ deg, $Re_{\infty,L} = 37.7 \times 10^6$).

wing length in a geometrically similar manner influences the radiation-adiabatic surface temperature.

Flowfield solutions are available for wing lengths $L_1 = 4.67$ m and $L_2 = 14$ m, thus, $L_1/L_2 = \frac{1}{3}$. All flow parameters are identical with the exception of the Reynolds number, which only varies due to the different wing lengths. The approximate theoretical ratio of the radiation-adiabatic wall temperature [Eq. (8)], amounts to $T_{ra,1}/T_{ra,2} = 1.147$. Therefore, it is expected that a smaller model, compared to the original size, undergoes higher thermal loads. The numerically determined ratio of the wall temperature, as well as the wall temperatures themselves, are plotted in Fig. 11 where the approximate theoretical value is also marked. On the windward side of the wing a fairly uniform temperature ratio prevails, except along a narrow zone at the symmetry plane. The difference to the theoretical value only amounts to about 2.5%, excellently confirming Eq. (8). The windward side of the wing essentially consists of two flat plates, obviously satisfying the boundary-layer assumptions. In contrast to this, the leeward side of the wing displays the whole spectrum of the temperature ratio $0.92 \leq T_{ra,1}/T_{ra,2} \leq 1.29$ immediately downstream of the leading edge.

The scaling is much improved, if Eq. (6) is used. It is evaluated directly, and with the assumption $\kappa_1 \approx \kappa_2$. The radiation-adiabatic wall temperature of the small wing is inserted in Eq. (6), which is solved for the radiation-adiabatic wall temperature of the large wing by way of a Newton iteration procedure. The result is plotted in Fig. 12. An excellent agreement concerning the radiation-adiabatic wall temperature between the scaled and the numerical value can now be obtained

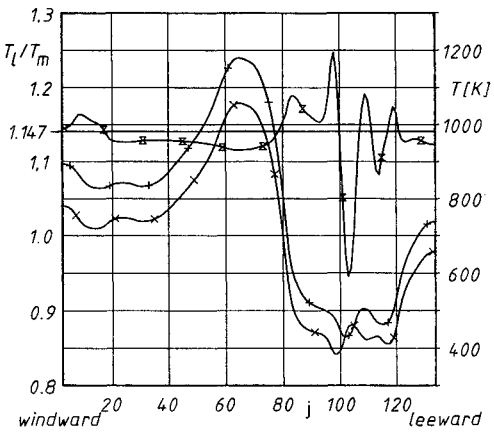

Fig. 11 Distributions of the wall temperature and the temperature ratio in the cross section $i = 120$ $T(L = 4.67)$: +, $T(L = 14$ m): ×, temperature ratio: ⧖.

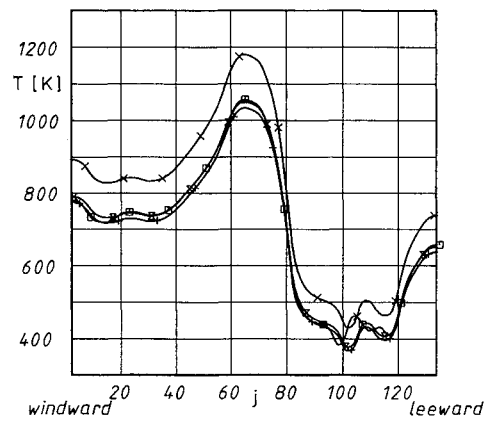

Fig. 12 Prediction of the radiation-adiabatic surface temperature in the cross section $i = 120$. ×: numerically given state 1 in Eq. (6) corresponds to a wing length $L = 4.67$ m; ⧖: result of Eq. (6) with condition Eq. (7b); +: result of Eq. (6); □: numerical result for state 2.

for most of the wing surface, especially with the assumption $\kappa_1 \approx \kappa_2$. Small deviations exist near the windward symmetry plane. A good agreement is also observed between the leeward symmetry plane and the separation line of the secondary vortices. The prediction of the temperature is relatively inaccurate between both separation lines, for reasons mentioned above.

As demonstrated here, a scaling of the radiation-adiabatic temperature is possible for laminar flow, if the flow is not too strongly three-dimensional, and if the flow topologies of the cases are similar (see also Ref. 4). However, with the present cold-surface wind-tunnel techniques, an experimental examination is not possible. If a very accurate and validated prediction is desired for design purposes, a hot experimental technique (HET) is necessary.[4]

Concluding Remarks

The viscous laminar flowfield past a delta wing with blunt leading edges has been numerically simulated to investigate the radiation-adiabatic (radiation-cooled adiabatic) surface temperature in a hypersonic flow. The perfect gas flow conditions are $M_\infty = 7.15$, $\alpha = 15$ deg, and altitude $H = 30$ km.

The general result, supported by analytical and numerical investigations, is that the radiation adiabatic temperature depends inversely on a characteristic boundary-layer thickness. For two-dimensional laminar flow, this scales with the Blasius thickness. Therefore, in general, the temperature at the windward side of the vehicle is much higher than on the leeward side. Attachment lines generally lead to hot-spot situations, while at separation lines rather low temperatures result.

Concerning the radiation-adiabatic surface temperature, there is a fair qualitative agreement on the windward side between the results obtained by an approximate method and a Navier-Stokes computation. The approximate method generally underpredicts the level of the surface temperature. This can be caused by the entropy-layer swallowing effect, which is neglected in the approximate method. At attachment lines, and also on the leeward side of an airplane, approximate methods should be used with caution. At the leeward side they need flow data, which cannot be provided by an inviscid computation, if separation is present.

The known radiation-adiabatic surface temperature on one wing can be transfered to another geometrically similar wing by means of a simple relation. This has been shown for the flow past two wings with identical freestream conditions. This is correct for regions where the flow is attached and not too strongly three-dimensional. If the flow is separated, it only holds if the topological structure of the separated flow is the same in both cases.

Only laminar flow was considered in this article in order to emphasize the basic effects. In principle, the findings are also valid for turbulent flow.

Acknowledgments

The work of A. Koç (MBB, München), who provided the result obtained with the approximate method, is highly appreciated. Special thanks are due to H. Vollmers (DLR, Göttingen) for the support with his high-performance three-dimensional graphic system comadi. S. Riedelbauch also thanks his colleagues at the DLR, Göttingen, for helpful discussions.

References

[1]Hirschel, E. H., "Heat Loads as Key Problem of Hypersonic Flight," *Zeitschrift für Flugwissenschaften und Weltraumforschung*, No. 76, Nov. 1992, pp. 349–356.

[2]Hoey, R. G., "AFFTC Overview of Orbiter-Reentry Flight-Test Results," *Shuttle Performance: Lessons Learned*, NASA CP 2283, Hampton, VA, March 1983, pp. 1303–1316.

[3]Bertin, J. J., and Goodrich, W. D., "Effects of Surface Temperature and Reynolds Number on Leeward Shuttle Heating," *Journal of Spacecraft and Rockets*, Vol. 13, No. 8, 1976, pp. 473–480.

[4]Hirschel, E. H., Koç, A., and Riedelbauch, S., "Hypersonic Flow

Past Radiation-Cooled Surfaces," AIAA Paper 91-5031, Dec. 1991.

[5]Koç, A., "Aerodynamische Aufheizung des Demonstrators," MBB GmbH, MBB/FE122/HYPAC/TN/0130, München, Germany, Nov. 1990.

[6]Pai, S., *Radiation Gas Dynamics*, Springer-Verlag, Wien, 1966, p. 1.

[7]Schlichting, H., "Grenzschicht-Theorie," Verlag G. Braun, Karlsruhe, 1965, pp. 243–290.

[8]Yee, H. C., "A Class of High-Resolution Explicit and Implicit Shock-Capturing Methods," von Karman Inst. Lecture Series 1989-04, Brussel, Belgium, March 6–10, 1989.

[9]Riedelbauch, S., "Aerothermodynamische Eigenschaften von Hyperschallströmungen über strahlungsadiabate Oberflächen," Ph.D. Dissertation, Technische Universität München, München, Germany, 1991, see also DLR-FB 91-42, Dec. 1991.

[10]Riedelbauch, S., and Brenner, G., "Numerical Simulation of Laminar Hypersonic Flow past Blunt Bodies Including High Temperature Effects," AIAA Paper 90-1492, June 1990.

[11]Riedelbauch, S., Brenner, G., Müller, B., and Kordulla, W., "Numerical Simulation of Laminar Hypersonic Flow past a Double-Ellipsoid," AIAA Paper 89-1840, June 1989.

[12]Riedelbauch, S., "Numerical Simulation of Laminar Hypersonic Flow past a Double-Ellipsoid," *Proceedings of the Workshop on Hypersonic Flows for Reentry Problems (Part I)*, Springer-Verlag, Berlin, Vol. 2, 1991, pp. 517–534.

[13]Riedelbauch, S., "Hypersonic Flow over a Delta Wing at High Angle of Attack," *Proceedings of the Workshop on Hypersonic Flows for Reentry Problems (Part II)*, Springer-Verlag, Berlin, Vol. 3, 1993, pp. 865–880.

[14]Riedelbauch, S., "Equilibrium Reactive Flow past the Double-Ellipsoid at $M_\infty = 25$," *Proceedings of the Workshop on Hypersonic Flows for Reentry Problems (Part II)*, Springer-Verlag, Berlin, Vol. 3, 1993, pp. 576–589.

[15]Linde, M., "Experimental Test on a Planar Delta Wing at High Mach Number and High Angle of Attack," Aeronautical Research Inst. of Sweden, TN 1988-59, Bromma, Sweden, Oct. 1988.

[16]Hirschel, E. H., "Evaluation of Results of Boundary-Layer Calculations with Regard to Design Aerodynamics," AGARD-R-741, April 1986, pp. 5-1–5-29.

[17]Peake, D. J., and Tobak, M., "Three-Dimensional Interactions and Vortical Flows with Emphasis on High Speeds," AGARDograph 252, March 1980.

[18]Anderson, J. D., "Hypersonic and High Temperature Gas Dynamics," McGraw-Hill, New York, 1989, pp. 295–297.